Proc. NIPR Symp. Antarct. Meteorites, 7, 110–124, 1994

CHEMICAL COMPOSITION OF Fe-Ni METAL AND PHOSPHATE MINERALS IN YAMATO-82094 CARBONACEOUS CHONDRITE

Yasuhiro SHIBATA and Hiroharu MATSUEDA

Department of Geology and Mineralogy, Faculty of Science, Hokkaido University, Kita-10 Nishi-8, Kita-ku, Sapporo 060

Abstract: The mineralogy of Fe-Ni metal and associated minerals in the Yamato (Y)-82094 carbonaceous chondrite (CO) have been studied by optical, scanning electron microscope and electron microprobe techniques. There are some characteristic features for the Fe-Ni metal in the Y-82094: (1) Ni contents in taenite grains are divided into two groups consisting of low- and high-Ni taenite. (2) Partition of Co between coexisting kamacite and taenite shows relatively higher temperatures (approximately 800°C), and their temperature ranges are wide. (3) polycrystalline taenite exists. (4) Fe-Ni metal and troilite form micron-sized intergrowths. (5) The Ni-Co trend of kamacite in chondrule is positive.

The high-Ni taenite could have formed through thermal metamorphism on the parent body, while low-Ni taenite might have formed due to reheating caused by shock metamorphism on the parent body or during the cooling process of chondrule formation. The positive Ni-Co trend of kamacite in Y-82094 is similar to that of the metal in CR chondrites. This trend may suggest that kamacite in Y-82094 preserves the primitive chemical composition indicating nebula condensation origin.

The Fe-Ni metal grains have many phosphate mineral inclusions (whitlockite, brianite and panethite). The mode of occurrence of brianite and panethite indicates that they might have formed simultaneously with the Fe-Ni metal in the nebula.

1. Introduction

The Yamato (Y)-82094 is a CO3 type chondrite (YANAI and KOJIMA, 1987), but SCOTT *et al.* (1992) reported that it is a unique type 3 carbonaceous chondrite. The shock effects in olivine and plagioclase suggest that Y-82094 underwent shock metamorphism on the parent body (SCOTT *et al.*, 1992). The petrologic subtype of Y-82094 is 3.5 according to the thermoluminescence sensitivity and other data (SEARS *et al.*, 1991), suggesting that Y-82094 has undergone weak metamorphism.

The main objective of this study is to clarify the formation process of Fe-Ni metal in Y-82094. We will describe the mode of occurrence and chemical composition of Fe-Ni metal and the associated minerals, and discuss the formation process and the possible origin of Fe-Ni metal.

2. Sample and Analytical Procedures

The samples studied here are Y-82094, Y-791717, Y-790992, and Y-81020. They are CO3 chondrites (YANAI and KOJIMA, 1987), in which Y-791717 and Y-81020 belong to petrologic subtype 3.3 (SEARS *et al.*, 1991).

All thin sections were observed under an optical microscope and a scanning electron microscope. Fe-Ni metal and sulfide minerals were analyzed with a wavelength dispersive electron microprobe analyzer (WDX, JEOL-Superprobe 733) at 15 kV accelerating voltage and 2–20 nA beam absorption on PCD. Co contents were corrected for the contribution of the Fe Kβ peak to the Co Kα peak by the estimated values using Fe-Ni metal grains with different compositions. Cu contents were also corrected for the contribution of Ni Kβ peak to the Cu Kα peak in the same manner. S contents were eliminated for the contribution of the Co Kα ($n=3$) peak to the S Kα peak by pulse height analysis. Phosphate minerals were analyzed with WDX and an energy dispersive electron microprobe analyzer (EDX, JED-2001) at 15 kV accelerating voltage and 4–10 nA. ZAF corrections were applied for measured X-ray relative intensity (YUI, 1992).

3. Results

The modes of occurrence of Fe-Ni metal are classified into three textural settings: (1) chondrule interior: Fe-Ni metal occurring within chondrule, (2) chondrule surface: Fe-Ni metal occurring in contact with matrix at the chondrule rim, and (3) matrix: Fe-Ni metal occurring in the matrix.

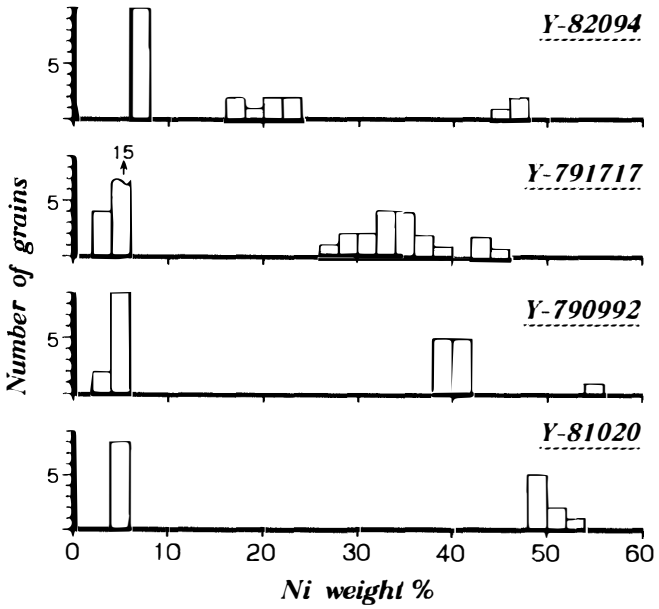

Fig. 1. Histograms of Ni contents in coexisting kamacite and taenite and/or tetrataenite in samples studied here. Ni contents in taenite grains of Y-82094 show a bimodal distribution.

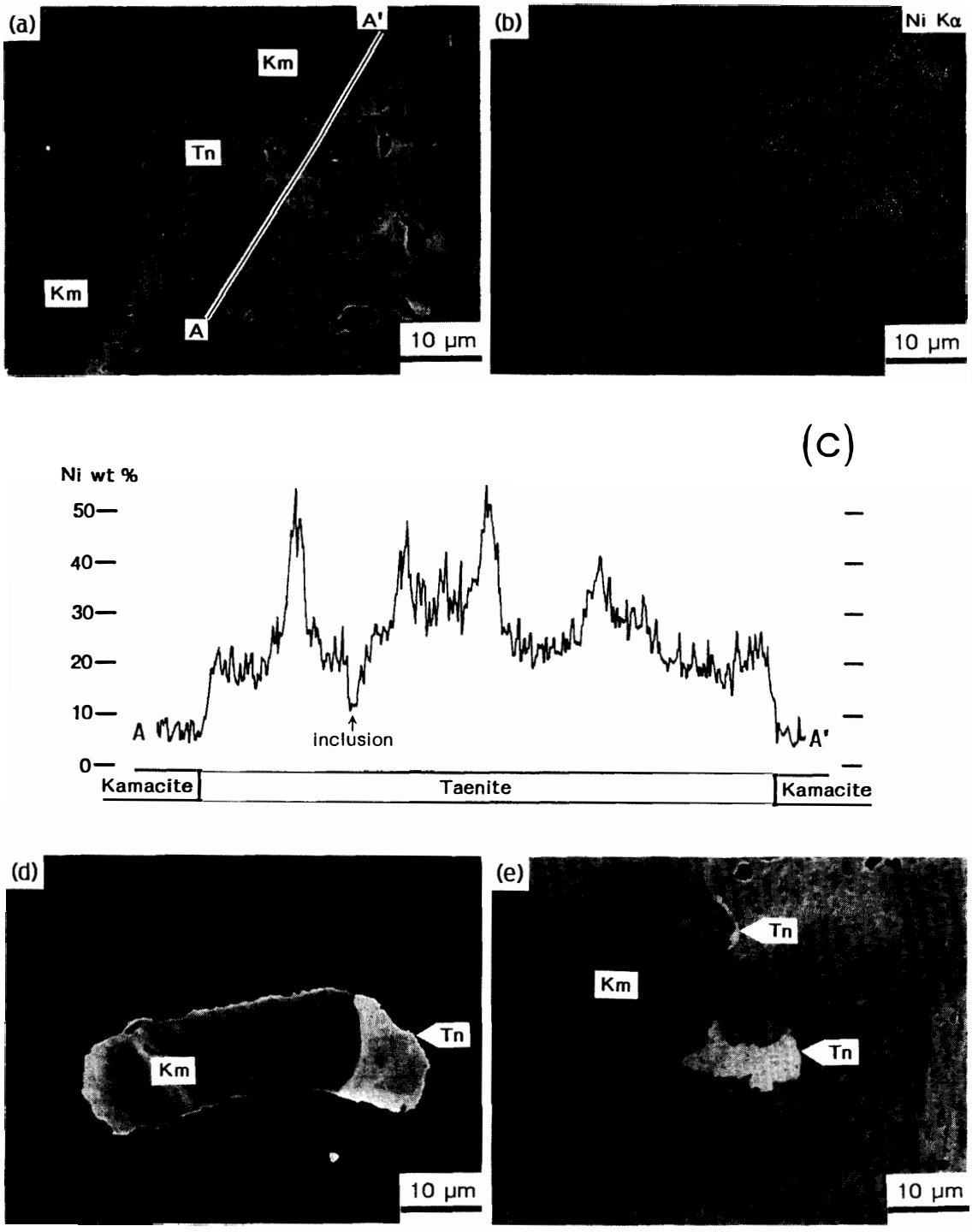

Fig. 2. The modes of occurrence of the Fe-Ni metal in Y-82094. (a) Backscattered electron image (BEI) of low-Ni taenite (Tn) coexisting with kamacite (Km) in the matrix. The inclusions (black) in taenite and kamacite are mostly chromite and phosphate minerals. (b) Characteristic X-ray image for Ni Kα, covering the same area (a). (c) Line profile for Ni Kα along section A–A′ in (a). (d) BEI of low-Ni taenite (Tn) coexisting with kamacite (Km) in chondrule interior. (e) BEI of high-Ni taenite (Tn) coexisting with kamacite (Km) in the matrix.

3.1. Fe-Ni metal

The major Fe-Ni metal in Y-82094 is kamacite, ranging from submicrometer to several hundred micrometers in size. Taenite is present in only small amount and coexists with kamacite and/or troilite. Fe-Ni metal in Y-82094 often includes coarse-grained phosphate and silicate minerals compared with other samples studied here. These mineral inclusions are rich in matrix metal, but poor in chondrule interior metal.

Figure 1 shows the Ni content in coexisting kamacite and taenite and/or tetrataenite. The chemical compositions of Fe-Ni metal are given in the appendix. Analyzed points for coexisting kamacite and taenite are near the grain boundary of both phases. The ordering of tetrataenite was not confirmed in this study. Here, we assume that the metal with over 49 wt% Ni is tetrataenite and that metal with 16–49 wt% Ni is taenite. The ranges of Ni contents of taenite grains in Y-791717, Y-790992 and Y-81020 are narrow, while those of taenite in Y-82094 are divided into two groups consisting of low- and high-Ni taenite.

Low-Ni taenite grains have 16–24 wt% Ni and are about 10–60 μm in diameter. Small low-Ni taenite is homogeneous in Ni content except in taenite rims adjacent to kamacite where Ni is enhanced (Fig. 2d). However, some larger low-Ni taenite grains are clearly heterogeneous in Ni. Figures 2a and 2b are the backscattered electron image and characteristic X-ray image of low-Ni taenite in kamacite, respectively. This low-Ni taenite grain seems to be polycrystalline and has narrow Ni-rich boundaries. These boundaries are only a few μm wide, occasionally with above 40 wt% Ni. Taenite rims adjacent to kamacite have slight enhancement of Ni

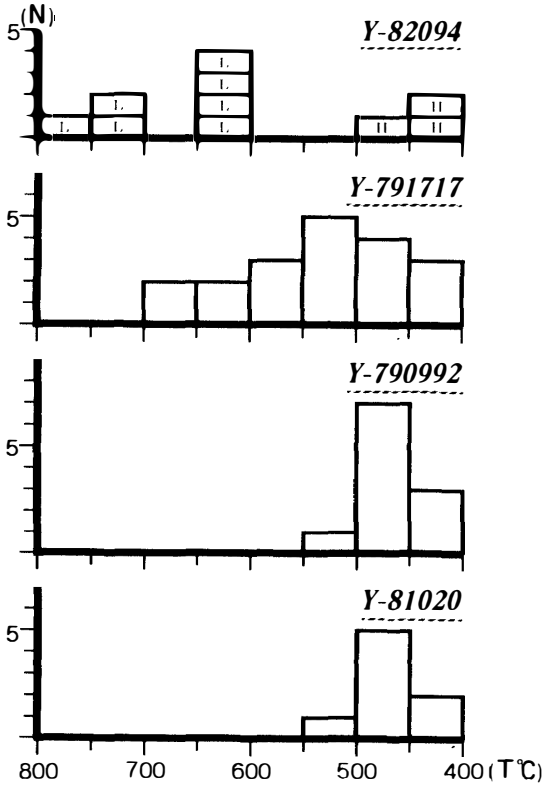

Fig. 3. Estimated temperatures based on the partition of Co between coexisting kamacite and taenite and/or tetrataenite. Estimation of temperature follows the method of AFIATTALAB *and* WASSON *(1980). "L" in the figure shows data for low-Ni taenite, while "H" shows data for high-Ni taenite. Y-82094 shows the higher temperatures and the wider range of temperature in comparison with other samples.*

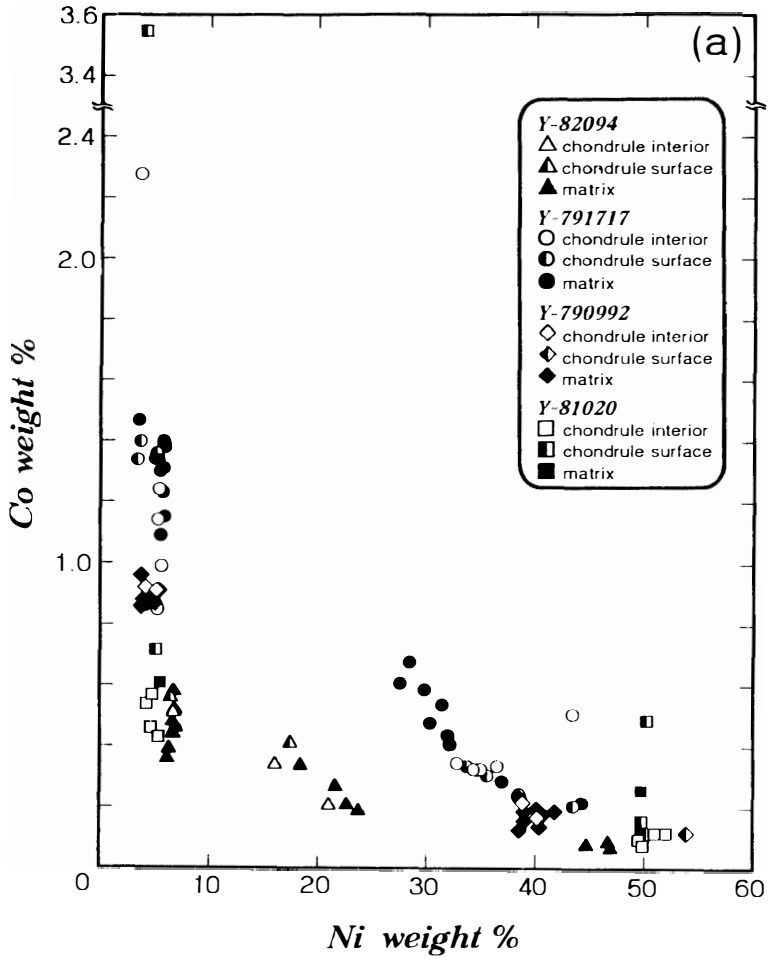
(a)
Y-82094
chondrule interior
chondrule surface
matrix
Y-791717
chondrule interior
chondrule surface
matrix
Y-790992
chondrule interior
chondrule surface
matrix
Y-81020
chondrule interior
chondrule surface
matrix
Co weight %
Ni weight %
3.6
3.4
2.4
2.0
1.0
0
10
20
30
40
50
60

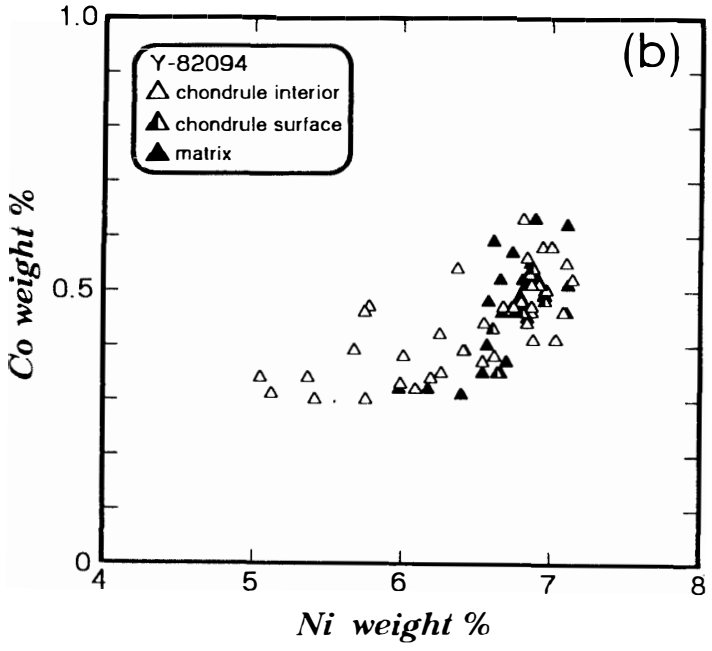
(b)
Y-82094
chondrule interior
chondrule surface
matrix
Co weight %
Ni weight %
1.0
0.5
0
4
5
6
7
8

Fig. 4.

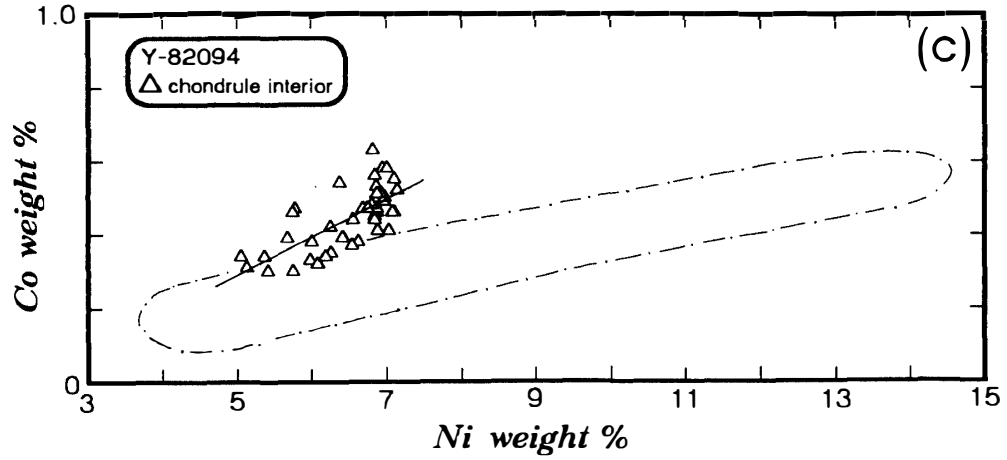

Fig. 4. (a) Plot of Ni vs. Co for coexisting kamacite and taenite and/or tetrataenite in Y-82094, Y-791717, Y-790992 and Y-81020. (b) Plot of Ni vs. Co for kamacite without taenite in Y-82094. (c) Plot of Ni vs. Co for kamacite without taenite in chondrule interior in Y-82094. The solid line shows the Ni-Co trend based on the least square method. The dashed loop shows the compositional range of the metal in CR chondrites according to WEISBERG *et al. (1988).*

as shown in Fig. 2c.

High-Ni taenite grains have about 45 wt% Ni and are about 10 μm in diameter. Those grains do not show heterogeneity of Ni (Fig. 2e). The low- and high-Ni taenite grains occur independently in chondrule interiors and the matrix.

Figure 3 shows estimated temperatures based on the partition of Co between coexisting kamacite and taenite, using the method of AFIATTALAB and WASSON (1980). In Y-82094, some Fe-Ni metal grains show higher temperatures, and the temperature range is wider than those of other samples. All low-Ni taenite grains show temperatures above 600°C, while all high-Ni taenite grains show temperatures below 500°C.

Figure 4a shows the plot of Ni vs. Co for coexisting kamacite, and taenite and/or tetrataenite. Co contents of kamacite in Y-82094 are about 0.4–0.6 wt%, while those of taenite are about 0.1–0.4 wt%. The Ni-Co trend in kamacite and taenite grains tends to show a negative correlation. Figure 4b shows the plot of Ni vs. Co for kamacite without taenite in Y-82094. Figure 4c shows the Ni-Co trend for kamacite only in chondrule interiors and the compositional range of metal in CR chondrites (WEISBERG *et al.*, 1988). Though Co contents in Y-82094 are higher than those of the metal of CR chondrites, the Ni-Co trend in kamacite grains in chondrule interiors has a positive correlation, which is similar to those of the metal of CR chondrites.

Phosphorus contents in Fe-Ni metal in Y-82094 are extremely low (below 0.03 wt%).

3.2. Troilite

Troilite intimately coexists with Fe-Ni metal or exists as isolated grains. Troilite

is abundant in the matrix, but scarce in chondrule interiors. The interfaces of troilite and Fe-Ni metal are mostly composed of micron-sized intergrowths of both phases (Fig. 5). The intergrowths were generally found in matrix metal. Table 1 shows the representative chemical compositions of troilite.

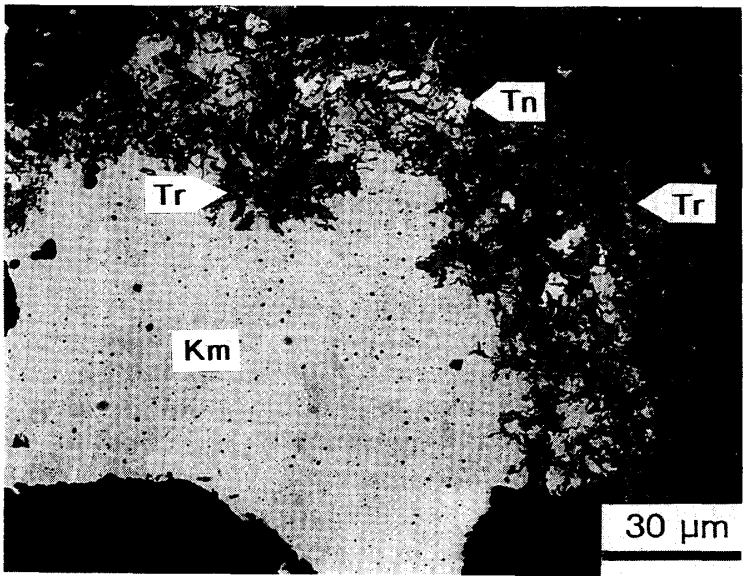

Fig. 5. Backscattered electron image of micron-sized intergrowths of troilite (Tr) and kamacite (Km). Fine-grained taenite (Tn) exists with troilite.

Table 1. Representative chemical compositions of troilite (1, 2, 3) and schreibersite (4, 5) in Y-82094.

wt%	1	2	3	4	5
Fe	62.69	62.37	62.29	44.14	48.29
Ni	0.02	0.14	0.04	39.33	36.14
Co	0.11	0.07	0.06	0.11	0.08
Cu	0.00	0.04	0.03	0.04	0.11
Cr	0.02	0.02	0.02	—	—
P	—	—	—	14.91	14.81
S	36.77	36.41	36.46	—	—
Total	99.61	99.05	98.90	98.53	99.43
atom%					
Fe	49.41	49.48	49.46	40.65	44.08
Ni	0.02	0.11	0.03	34.46	31.39
Co	0.08	0.06	0.05	0.10	0.07
Cu	0.00	0.03	0.02	0.03	0.09
P	—	—	—	24.76	24.37
S	50.48	50.31	50.42	—	—

3.3. Phosphate minerals and schreibersite

Kamacite in the matrix of Y-82094 generally includes phosphate minerals (typically $<20\,\mu$m in size). They are mostly whitlockite, only a few Na-rich phosphate minerals such as brianite and panethite are encountered. Chemical compositions of phosphate minerals are shown in Table 2. Figure 6 shows back-

Table 2. Representative chemical compositions of whitlockite, brianite and panethite in Y-82094 (whitlockite by WDX, brianite and panethite by EDX).

	Whitlockite	Brianite	Panethite
wt%			
CaO	45.2	18.2	0.2
MgO	3.2	11.1	14.6
FeO	3.2	3.5	18.2
Na_2O	2.9	20.0	21.2
MnO	—	—	1.0
Cr_2O_3	0.3	—	—
P_2O_5	45.0	47.2	44.8
Total	99.8	100.0*	100.0*
ions	at O=28	at O=8	at O=8
Ca	8.79	0.99	0.01
Mg	0.87	0.84	1.13
Fe	0.49	0.15	0.79
Na	1.02	1.96	2.14
Mn	—	—	0.04
Cr	0.04	—	—
P	6.91	2.02	1.98
Σ	18.12	5.96	6.09

* Normalized data.

scattered electron image and characteristic X-ray images of P, Ca and Na Kα for phosphate minerals in kamacite.

Whitlockite exists as inclusions in all samples with variable grain size and abundance, while brianite and panethite are found only in Y-82094. Whitlockite in Y-82094 usually exists in kamacite, occasionally in contact with silicate minerals in the matrix. This whitlockite occurs along external surfaces of kamacite grains and is rounded in shape. Brianite and panethite showing euhedral or fragmental shape in the central part of kamacite grains coexist only with kamacite, taenite and troilite.

Schreibersite is very small in amount and coexists with kamacite in chondrule interiors, but not with any other minerals. Chemical compositions of schreibersite are shown in Table 1.

4. Discussion

4.1. Formation process of Fe-Ni metal in Y-82094

The characteristic features for Fe-Ni metal in Y-82094 are summarized as follows: (1) Bimodal distributions of Ni contents in taenite grains. (2) Higher and wider temperature range, in comparison with Fe-Ni metals in other CO chondrites. (3) Existence of polycrystalline taenite. (4) Micron-sized intergrowths of kamacite and troilite at the interface. (5) The positive Ni-Co trend is similar to that of the metal in CR chondrites. We discuss the formation process of Fe-Ni metal in Y-82094 on the basis of the above-mentioned features.

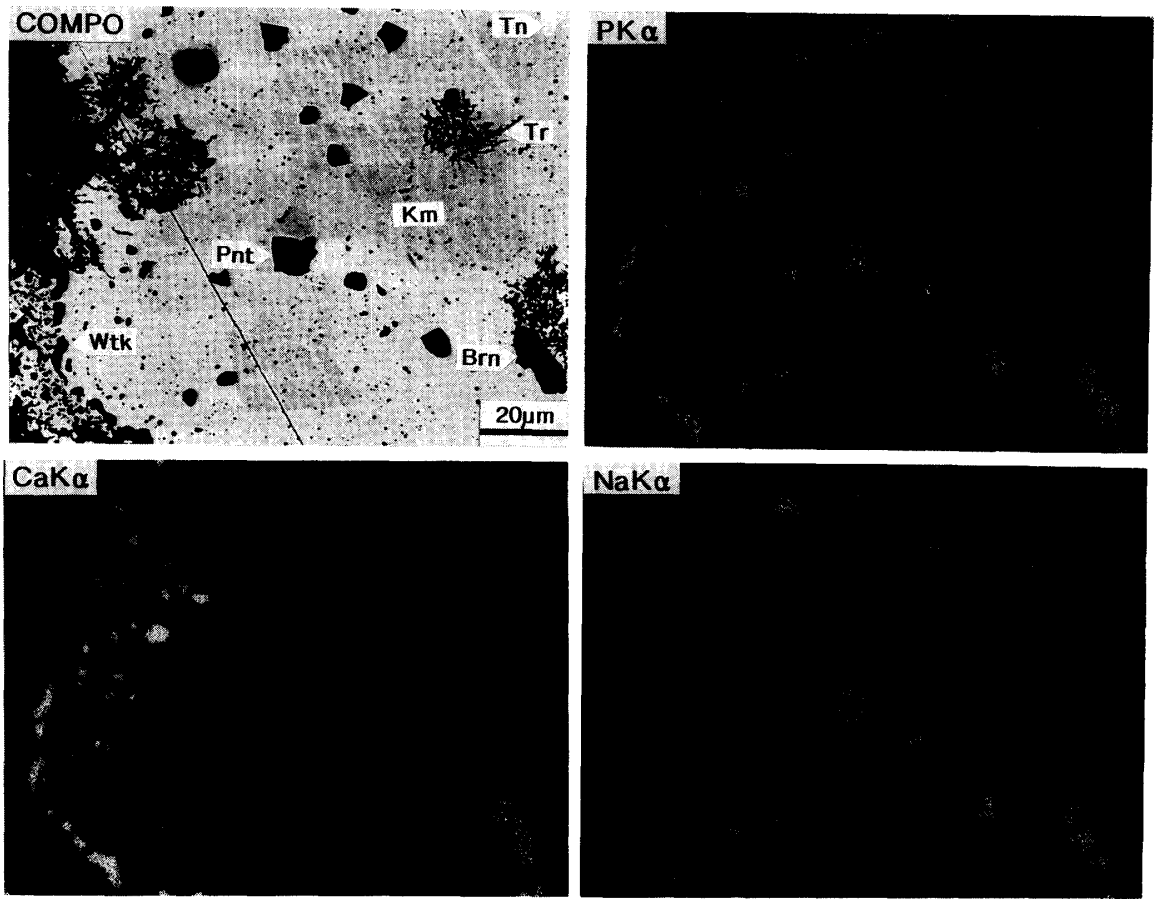

Fig. 6. Backscattered electron image and characteristic X-ray images for the P, Ca and Na Kα line of phosphate minerals in kamacite grains. Whitlockite (Wtk) grains exist in the marginal parts of kamacite (Km) grains near the surrounding matrix, while brianite (Brn) and panethite (Pnt) exist in the central part of kamacite. They do not contact any minerals except kamacite (Km), taenite (Tn) and troilite (Tr). All images are the same scale.

BEVAN and AXON (1980) suggested that polycrystalline taenite in Tieschitz (H 3 chondrite) is a relict of a primary solidification structure from Fe-Ni melt, and compositional heterogeneities of Ni were produced by rapid, non-equilibrium cooling of Fe-Ni melt during chondrule formation. The mode of occurrence of polycrystalline taenite in Y-82094 is similar to that in Tieschitz except for the degree of enhancement of Ni in kamacite/taenite grain boundaries. The polycrystalline taenite in Y-82094 is not produced by solidification from Fe-Ni melt on the parent body. Y-82094 underwent weak shock metamorphism (shock pressure: 5–10 GPa, post-shock temperature increase: 20–50°C, SCOTT *et al.*, 1992), and the post-shock temperature did not reach the melting temperature of Fe-Ni metal. Besides, the polycrystalline taenite is not produced by diffusion controlled growths of kamacite and taenite during slow cooling below 900°C. Thus, the polycrystalline taenite in Y-82094 is also a relict of a primary solidification structure during chondrule formation.

The low-Ni taenite grains showing higher temperatures might have experienced

rapid cooling. It is generally accepted that plessite and/or martensite form as a result of rapid cooling, but those phases do not exist in our thin section. This may indicate that the cooling rates of low-Ni taenite grains are lower than those of plessite and/or martensite.

The formation stage of low-Ni taenite depends on how the micron-sized intergrowths of Fe-Ni metal and troilite are formed.

SCOTT *et al.* (1992) pointed out that Y-82094 underwent shock metamorphism, which was classified as shock stage 2. They found micron-sized intergrowths of Fe-Ni metal and polycrystalline troilite in the Lancé (CO3), which underwent less shock metamorphism than Y-82094. They hypothesized that intergrowths of both phases appear to result from local melting and rapid recrystallization caused by weak shock metamorphism. Apparently, the intergrowths of Fe-Ni metal and troilite in Y-82094 are similar to those in Lancé. Assuming the same mechanism for intergrowths in Y-82094 in spite of the relatively weak degree of shock, it is concluded that Fe-Ni metal in Y-82094 was affected by shock metamorphism. Considering reheating by shock metamorphism, Fe-Ni metal might cause a phase transition and compositional change, because the Fe-Ni-S eutectic temperature is 950–1000°C (SMITH and GOLDSTEIN, 1977). The heating caused compositional change in relatively weak degree, because of Ni in polycrystalline taenite remains heterogeneous after heating. Thus, the low-Ni taenite grain and low-Ni parts in polycrystalline taenite could have formed on the parent body as a result of subsequent rapid cooling after shock heating.

An alternative formation process of intergrowths of Fe-Ni metal and troilite is reaction of metal and gaseous sulfur in the nebula. In this case, precursor material of Fe-Ni metal experienced brief heating and rapid cooling during chondrule formation. The low-Ni taenite could have formed during cooling.

On the other hand, the high-Ni taenite could have formed through thermal metamorphism on the parent body (irrespective of the formation process of the low-Ni taenite). JONES and RUBIE (1991) estimated that the peak metamorphic temperature is about 500°C on the CO3 parent body. Temperatures of high-Ni taenite based on the partition of Co are 400–500°C and overlap the values estimated by JONES and RUBIE (1991). The thermal metamorphism on the parent body could also affect the low-Ni taenite grains (*e.g.* the enhancement of Ni in rims of low-Ni taenite adjacent to kamacite). However, these rims are very narrow, a few microns to submicrons wide, and have small enhancement of Ni (Fig. 1c). Indeed, thermal metamorphism might affect the composition of low-Ni taenite, but the effect could be limited due to sluggish diffusion of Ni under the low temperatures. Assuming that low-Ni taenite grains were produced by shock metamorphism, the high-Ni taenite grains could form through thermal metamorphism after shock metamorphism. If the high-Ni taenite had already existed before the shock event, low Ni content parts would form in high-Ni taenite rims adjacent to kamacite. However, those parts are not present.

Finally, the chemical composition of kamacite is an important feature revealing the origin of Fe-Ni metal of Y-82094. WEISBERG *et al.* (1988) suggested that the

Ni-Co trend for Fe-Ni metal in ALH-85085 overlaps that of metal in CR chondrites and is similar to a nebular condensation path calculated by GROSSMAN and OLSEN (1974). In Y-82094 kamacite coexisting with taenite has a narrow compositional range of Ni (Fig. 4a), on the contrary, kamacite without taenite in chondrule interiors has a wider compositional range of Ni (Fig. 4b). Though kamacite and taenite grains in Y-82094 have a negative Ni-Co trend like that of metal in metamorphosed ordinary chondrites, kamacite grains in chondrule interiors alone in Y-82094 have a positive Ni-Co trend like that of Fe-Ni metal in primitive carbonaceous chondrites (*e.g.* CR chondrites). Compared with the slope of Ni-Co correlation in the metal in CR chondrites, the slope of kamacite in chondrule interiors in Y-82094 is slightly different (Fig. 4c). Moreover, CR chondrites generally contain martensite (*e.g.* LEE *et al.*, 1992), while Y-82094 does not contain martensite. We do not have a clear interpretation for the differences between the Fe-Ni metals in Y-82094 and in CR chondrites. However, it is possible that pre-existing martensite in Y-82094 before a shock event might decompose into kamacite and low-Ni taenite in shock heating. In summarizing the above discussions, we suggest that Fe-Ni metal in Y-82094 may have features of both the primitive Fe-Ni metal and the metamorphosed metal.

4.2. Formation of phosphate minerals

Many processes have been proposed for the formation of phosphate minerals accompanied by Fe-Ni metal. RUBIN and GROSSMAN (1985) suggested that phosphate minerals with Fe-Ni metal have been formed by a reaction of phosphide and/or phosphorus in the metal and calcium from matrix minerals. As shown in Fig. 6, whitlockite grains in Y-82094 exist in the rims of kamacite, occasionally coexisting with surrounding matrix minerals. These modes of occurrence are very similar to that of the phosphate-metal assemblage shown by RUBIN and GROSSMAN (1985). Therefore, the formation process of whitlockite in Y-82094 may be the process suggested by RUBIN and GROSSMAN (1985).

FUCHS *et al.* (1967) proposed that Na-rich phosphate minerals such as brianite and panethite in iron meteorites have been formed by the reaction among coexisting minerals (albite, enstatite, schreibersite and metal). WLOTZKA (1976) proposed that brianite and "Fe-panethite" in sulfide (troilite and pentlandite) were formed by introduction of sodium from Ca-Al-rich inclusions during a late metasomatic process in the Allende meteorite after condensation and agglomeration.

Brianite and panethite in Y-82094 do not coexist with any other minerals providing Na, Mg and Ca. Consequently brianite and panethite in Y-82094 are probably not the products of reaction among coexisting minerals. A possible formation process of Na-rich phosphate minerals is the reaction between phosphide and/or phosphorus in the metal and the gas phase of Na, Mg and Ca, or direct condensation products. Brianite and panethite are completely surrounded by Fe-Ni metal, therefore Na-rich phosphates might have formed during condensation of the Fe-Ni metal in the nebula, not the reactions on the parent body.

5. Conclusions

Y-82094 has low-Ni taenite and high-Ni taenite coexisting with kamacite. The high-Ni taenite could have formed through thermal metamorphism on the parent body, while the low-Ni taenite might have formed through shock metamorphism on the parent body or rapid cooling in the process of chondrule formation. It is possible that the polycrystalline taenite is a relict of solidification from Fe-Ni melt during chondrule formation. Kamacite and taenite grains in Y-82094 show a negative Ni-Co trend as does the metal in metamorphosed ordinary chondrite. However, only kamacite grains within chondrules show a positive Ni-Co trend which is similar to the trend of the metal in CR chondrites. The Ni-Co trend of kamacite in Y-82094 suggests that kamacite in Y-82094 preserves the primitive chemical composition indicating nebula condensation origin. The Fe-Ni metal in Y-82094 contains many phosphate inclusions (whitlockite, brianite and panethite). The modes of occurrence of brianite and panethite indicate that these minerals might have formed in the nebula.

Acknowledgments

The authors are indebted to Drs. K. YANAI and H. KOJIMA, National Institute of Polar Research, for the meteorite samples. We thank Prof. S. YUI of Hokkaido University for his discussions and Mr. S. TERADA of Hokkaido University for his help in EPMA operation.

References

AFIATTALAB, F. and WASSON, J. T. (1980): Composition of the metal phases in ordinary chondrites: Implications regarding classification and metamorphism. Geochim. Cosmochim. Acta, **44**, 431–446.

BEVAN, A. W. R. and AXON, H. J. (1980): Metallography and thermal history of the Tieschitz unequilibrated meteorite—metallic chondrules and the origin of polycrystalline taenite. Earth Planet. Sci. Lett., **47**, 353–360.

FUCHS, L. H., OLSEN, E. and HENDERSON, E. P. (1967): On the occurrence of brianite and panethite, two new phosphate minerals from the Dayton meteorite. Geochim. Cosmochim. Acta, **31**, 1711–1719.

GROSSMAN, L. and OLSEN, E. (1974): Origin of the high-temperature of C2 chondrites. Geochim. Cosmochim. Acta, **38**, 173–187.

JONES, R. H. and RUBIE, D. C. (1991): Thermal metamorphism of CO3 chondrites: Application of olivine diffusion modelling to parent body metamorphism. Earth Planet. Sci. Lett., **106**, 73–86.

LEE, M. S., RUBIN, A. E. and WASSON, J. T. (1992): Origin of metallic Fe-Ni in Renazzo and related chondrites. Geochim. Cosmochim. Acta, **56**, 2521–2533.

RUBIN, A. E. and GROSSMAN, J. N. (1985): Phosphate-sulfide assemblages and Al/Ca ratios in type-3 chondrites. Meteoritics, **20**, 479–489.

SCOTT, E. R. D., KEIL, K. and STÖFFLER, D. (1992): Shock metamorphism of carbonaceous chondrites. Geochim. Cosmochim. Acta, **56**, 4281–4293.

SEARS, D. W. G., BATCHELOR, J. D., LU, J. and KECK, B. D. (1991): Metamorphism of CO and

CO-like chondrites and comparisons with type 3 ordinary chondrites. Proc. NIPR Symp. Antarct. Meteorites, **4**, 319–343.

SMITH, B. A. and GOLDSTEIN, J. I. (1977): The metallic microstructures and thermal histories of severely reheated chondrites. Geochim. Cosmochim. Acta, **41**, 1061–1072.

WEISBERG, M. K., PRINZ, M. and NEHRU, C. E. (1988): Petrology of ALH85085: A chondrite with unique characteristics. Earth Planet. Sci. Lett., **91**, 19–32.

WLOTZKA, F. (1976): Phosphates in the Allende carbonaceous chondrite. Meteoritics, **11**, 393–394.

YANAI, K. and KOJIMA, H. (1987): Photographic Catalog of the Antarctic Meteorites. Tokyo, Natl Inst. Polar Res., 298 p.

YUI, S. (1992): A system of EPMA data reduction programs using BASIC for personal computer in 1992. J. Fac. Sci., Hokkaido Univ., **23**(2), 147–158.

(Received August 9, 1993; Revised manuscript received December 16, 1993)

Appendix

Chemical composition of coexisting kamacite, and taenite and/or tetrataenite in all studied samples. Same numbers indicate the paired Fe-Ni metal grains. I, S and M indicate the textural setting of Fe-Ni metal as chondrule interior, chondrule surface and matrix, respectively.

Y-82094									
No.	Pos.	Fe	Ni	Co	Cu	Cr	P	S	Total
1	M	77.68	21.70	0.27	0.13	0.17	0.01	0.03	99.99
1		92.22	6.92	0.58	0.00	0.24	0.00	0.00	99.96
2	M	53.97	46.74	0.09	0.39	0.11	0.00	0.02	101.32
2		93.10	6.46	0.39	0.02	0.29	0.00	0.00	100.26
3	M	76.71	22.81	0.21	0.10	0.52	0.01	0.04	100.40
3		92.43	7.01	0.52	0.02	0.11	0.00	0.00	100.09
4	M	75.80	23.89	0.19	0.13	0.20	0.00	0.00	100.21
4		92.76	7.04	0.46	0.03	0.10	0.01	0.00	100.40
5	I	83.00	16.18	0.34	0.09	0.18	0.00	0.00	99.79
5		91.31	6.98	0.52	0.00	0.44	0.01	0.01	99.27
6	S	82.60	17.56	0.41	0.09	0.06	0.00	0.02	100.74
6		92.86	6.65	0.56	0.00	0.22	0.02	0.02	100.33
7	S	78.64	21.14	0.21	0.08	0.05	0.02	0.03	100.17
7		92.19	6.89	0.51	0.05	0.03	0.01	0.02	99.70
8	I	80.59	18.50	0.34	0.12	0.56	0.00	0.12	100.23
8		91.33	6.81	0.48	0.03	0.66	0.03	0.02	99.36
9	M	54.54	44.78	0.08	0.39	0.07	0.00	0.04	99.90
9		91.75	6.82	0.44	0.03	0.75	0.00	0.00	99.79
10	M	50.43	47.01	0.07	0.43	0.86	0.00	0.07	98.87
10		94.80	6.31	0.36	0.01	0.21	0.00	0.00	101.69
Y-791717									
No.	Pos.	Fe	Ni	Co	Cu	Cr	P	S	Total
1	M	65.81	32.09	0.44	0.21	0.35	0.02	0.00	98.92
1		92.87	5.51	1.30	0.01	0.49	0.03	0.02	100.23
2	M	55.02	44.33	0.22	0.32	0.00	0.01	0.02	99.92
2		93.88	5.37	1.34	0.00	0.01	0.02	0.00	100.62
3	M	65.29	34.82	0.33	0.19	0.02	0.00	0.01	100.66
3		94.95	5.76	1.23	0.00	0.00	0.01	0.01	101.96

4	M	66.77	30.42	0.48	0.12	0.80	0.00	0.00	98.59
4		94.07	3.57	1.47	0.00	0.60	0.01	0.00	99.72
5	I	64.19	35.11	0.33	0.17	0.04	0.00	0.03	99.87
5		92.94	5.69	0.99	0.00	0.01	0.00	0.01	99.64
6	M	68.97	31.55	0.54	0.20	0.29	0.00	0.01	101.56
6		94.45	5.87	1.38	0.03	0.04	0.00	0.00	101.77
7	I	53.89	43.53	0.51	0.30	0.48	0.00	0.22	98.93
7		92.72	3.60	2.28	0.04	0.48	0.01	0.03	99.16
8	M	69.34	29.90	0.59	0.11	0.00	0.01	0.02	99.97
8		93.18	5.95	1.38	0.00	0.00	0.00	0.01	100.52
9	I	61.85	36.63	0.34	0.23	0.15	0.02	0.00	99.22
9		95.08	5.46	1.24	0.00	0.05	0.01	0.00	101.84
10	S	59.55	38.64	0.25	0.24	0.21	0.01	0.01	98.91
10		93.28	5.08	1.34	0.03	0.14	0.04	0.00	99.91
11	M	62.99	37.04	0.29	0.24	0.08	0.00	0.01	100.65
11		93.71	5.79	1.40	0.05	0.09	0.00	0.02	101.06
12	M	66.36	32.30	0.41	0.16	0.32	0.00	0.03	99.58
12		94.44	5.56	1.09	0.03	0.01	0.00	0.01	101.14
13	S	61.64	35.69	0.31	0.26	0.68	0.03	0.04	98.65
13		94.01	3.48	1.34	0.02	0.49	0.00	0.03	99.37
14	I	67.13	32.88	0.35	0.21	0.05	0.00	0.02	100.64
14		93.75	5.30	0.85	0.03	0.04	0.01	0.02	100.00
15	I	65.34	34.43	0.33	0.26	0.00	0.00	0.01	100.37
15		93.73	5.34	1.14	0.00	0.00	0.02	0.00	100.23
16	S	64.99	33.79	0.34	0.22	0.33	0.00	0.01	99.68
16		94.93	3.77	1.40	0.00	0.02	0.00	0.00	100.12
17	M	71.58	28.52	0.68	0.18	0.02	0.02	0.01	101.01
17		93.61	5.82	1.31	0.06	0.01	0.00	0.00	100.81
18	S	54.45	43.60	0.21	0.33	0.02	0.00	0.01	98.62
18		93.89	5.20	1.36	0.01	0.03	0.02	0.00	100.51
19	M	71.14	27.66	0.61	0.15	0.00	0.00	0.01	99.84
19		93.49	5.91	1.15	0.02	0.01	0.02	0.00	100.60

Y-790992

No.	Pos.	Fe	Ni	Co	Cu	Cr	P	S	Total
1	M	60.36	38.64	0.24	0.21	0.02	0.00	0.01	99.48
1		94.62	5.31	0.91	0.06	0.01	0.01	0.02	100.94
2	M	58.78	40.87	0.18	0.34	0.15	0.00	0.03	100.35
2		95.06	4.42	0.87	0.00	0.04	0.00	0.00	100.39
3	M	59.39	40.20	0.20	0.33	0.05	0.02	0.01	100.20
3		93.16	5.11	0.87	0.03	0.07	0.00	0.00	99.24
4	S	46.67	54.01	0.12	0.24	0.01	0.00	0.01	101.06
4		94.42	5.45	0.91	0.00	0.02	0.01	0.02	100.83
5	M	57.45	40.48	0.14	0.34	0.54	0.03	0.04	99.02
5		93.69	4.61	0.91	0.01	0.59	0.00	0.02	99.83
6	M	57.29	41.88	0.19	0.35	0.03	0.00	0.00	99.74
6		94.54	3.84	0.86	0.03	0.03	0.00	0.02	99.32
7	M	61.10	39.11	0.16	0.22	0.00	0.00	0.01	100.60
7		94.89	4.22	0.87	0.00	0.05	0.02	0.01	100.06
8	I	57.83	40.29	0.17	0.31	0.48	0.00	0.03	99.11
8		93.62	4.22	0.92	0.01	0.38	0.00	0.02	99.17
9	M	61.00	39.10	0.19	0.30	0.02	0.01	0.00	100.62
9		95.53	3.83	0.96	0.00	0.01	0.00	0.00	100.33

10	I	60.25	38.98	0.22	0.27	0.04	0.02	0.01	99.79
10		93.75	5.24	0.91	0.07	0.04	0.00	0.00	100.01
11	M	60.49	38.63	0.13	0.32	0.02	0.00	0.03	99.62
11		94.86	4.00	0.88	0.04	0.16	0.00	0.02	99.96

Y-81020

No.	Pos.	Fe	Ni	Co	Cu	Cr	P	S	Total
1	I	49.04	49.57	0.10	0.13	0.59	0.00	0.02	99.45
1		94.31	4.77	0.46	0.00	0.57	0.00	0.04	100.15
2	M	50.25	49.79	0.12	0.20	0.13	0.00	0.03	100.52
2		94.59	5.62	0.61	0.01	0.19	0.00	0.01	101.03
3	S	47.85	49.87	0.16	0.23	0.19	0.00	0.01	98.31
3		92.97	5.20	0.72	0.03	0.04	0.05	0.04	99.05
4	I	47.79	51.06	0.12	0.21	0.44	0.01	0.04	99.67
4		93.23	5.47	0.43	0.00	0.41	0.00	0.02	99.56
5	I	49.24	49.98	0.08	0.14	0.09	0.01	0.03	99.57
5		95.32	4.36	0.54	0.00	0.10	0.00	0.00	100.32
6	I	46.47	52.11	0.12	0.22	0.36	0.00	0.03	99.31
6		93.48	4.90	0.57	0.03	0.37	0.21	0.02	99.58
7	M	47.83	49.81	0.26	0.18	0.00	0.03	0.03	98.14
7		93.05	5.21	1.34	0.00	0.01	0.14	0.01	99.76
8	S	48.28	50.39	0.49	0.18	0.00	0.03	0.02	99.39
8		92.69	4.17	3.56	0.00	0.02	0.00	0.00	100.44